

Journal of Engineering Technology and Applied Physics

Mesh Convergence Analysis on The Aerodynamic Performance of A Sedan Vehicle

Afzatul Najwa Nor Azman¹, Kausalyah Venkatasen^{1,*} and Shastri Sivaguru²

¹*School of Mechanical Engineering, College of Engineering, Universiti Teknologi MARA, 40450 Selangor Darul Ehsan, Malaysia.*

²*School of Engineering & Physical Sciences, Heriot Watt University Malaysia, Precinct 5, Putrajaya, 62200 Wilayah Persekutuan Putrajaya, Malaysia.*

*Corresponding author: kausalyah@uitm.edu.my, ORCID: 0000-0001-9707-0782

<https://doi.org/10.33093/jetap.2025.7.1.14>

Manuscript Received: 27 January 2025, Accepted: 3 March 2025, Published: 15 March 2025

Abstract — This article performs a comprehensive mesh convergence analysis on the aerodynamic efficiency of sedan vehicles. Leading CAD and CFD tools, such as CATIA and ANSYS Fluent are used to model the geometry and run the aerodynamic simulations. The simulations are centred on evaluating the drag coefficient (Cd) for four different sedan profiles. A full scale and half scale profile model configuration were used to analyse and assess the simulations' impact precision and computational efficiency. A thorough mesh sensitivity investigation is conducted to determine the effect and influence of the element sizing on Cd precision and processing time. The finding points to an element size of 0.5 m, as the optimal choice offering a balance between computational resource efficacy and precision on aerodynamic predictions. The full-scale model reduces the computational time significantly without compromising accuracy hence making it the selected choice for the aerodynamic simulations. The findings of this study underscore the importance of selecting an appropriate mesh element size for vehicle aerodynamic model. This study recommends a 0.5 m element size for future aerodynamic evaluations, thereby improving the equilibrium between simulation accuracy and computational cost in sedan aerodynamics.

Keywords— Frontal impact, Sedans, Drag coefficient, Mesh convergence, Processing time.

I. INTRODUCTION

Aerodynamics of the vehicle has always been a main concern where significant effort has gone toward optimizing the drag coefficient (Cd) which is a fundamental factor influencing stability and energy economics. By allowing thorough flows with intricate geometries, computational fluid dynamics (CFD) has also become a main instrument for aerodynamics research and optimization in vehicles. The past literature by Connolly *et al.* [1] demonstrated that vehicle aerodynamic characteristics are critical to

reducing fuel consumption as well as improving the performance of modern vehicles, especially for a sedan, which is still one of the most popular vehicle types in the world.

One of the most important parameters affecting the accuracy of CFD simulations is the quality of the computational mesh. It was found by Schlipf *et al.* and Celik *et al.* [2, 3] that mesh resolution and refinement are very important for getting accurate simulation results, especially for important values like Cd. Mesh convergence analysis is a standard technique for confirming the numerical accuracy by ensuring that additional refinement of the mesh does not yield a significantly different output. Researchers Mohamad *et al.* [4] pointed out that mesh refinement should be carried out before any results can be really considered consistent or reliable, and therefore, mesh convergence should be the first step of any CFD study.

Prabowo *et al.* and Ghavidel *et al.* [5, 6] have presented samples for automotive studies. Aerodynamic studies that optimize the drag coefficient emphasize the necessity of mesh convergence. Techniques to analyse convergence errors due to mesh in CFD simulations were described in detail by Shah [7] and further justified by Bupalov *et al.* [8] in which implementations of the specifications are numerically reliable even when there are no exact solutions that can be determined.

Although an extensive amount of study on vehicle aerodynamics was done, most studies have concentrated mostly on lowering aerodynamic drag by means of additional features or on investigating particular frontal factors, as in the works of Gao and Vignesh *et al.* [9, 10], moreover extensive mesh convergence analysis was not present in these past researches.

Building on earlier research, this work methodically investigates mesh convergence with

relation to sedan aerodynamics. For better understanding of how mesh resolution affects Cd predictions, changing mesh sizes in CFD models is likened to finding the right balance between both speed and precision. This work provides a disciplined way for next parametric research of vehicle front-end designs by using the Design of Experiments (DoE) method. This work aims to provide a more uniform strategy for mesh refinement in vehicle before embarking on detailed aerodynamic analysis.

II. MATERIALS AND METHODS

A. Vehicle Front End Parameter Selection

This study focuses on identifying the parameters that contribute to the aerodynamic performance in the vehicle design. Based on past research by Kausalyah *et al.* and Mizuno [11, 12], these frontal parameters are the most crucial elements under investigation using the Central Composite Design (CCD) approach. Seven key parameters related to modelling the frontal geometry of vehicles were included: bumper lead (BL), bumper centre height (BCH), hood leading edge (HLE), hood length (HL), windshield angle (WSi), hood angle (Hα) and hood edge height (HEH). A display of the seven parameters is exhibited in Fig. 1, which portrays the necessities for assessment, and the parametric specification is demonstrated in Table I.

Table I. Parameter table (mm, degrees).

x	Parameter	
x ₁	WSα (Degrees)	Windshield Angle
x ₂	BL	Bumper Lead
x ₃	BCH	Bumper Centre Height
x ₄	HLE	Hood Leading Edge
x ₅	HL	Hood Length
x ₆	Hα (Degrees)	Hood Angle
x ₇	HEH	Hood Edge Height

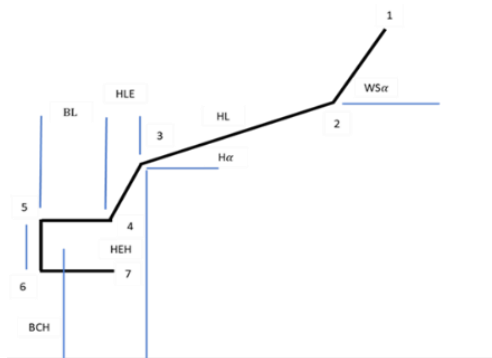


Fig. 1. Seven parameters of sedan vehicle.

Kausalyah *et al.* and Mizuno conducted a parametric analysis of the vehicle's front-end profile utilizing seven parameters; nonetheless, their influence on aerodynamic efficiency remains inadequately assessed [11, 12]. Therefore, these same parameters have been returned in this study to assess their impact on aerodynamic performance, hence the necessity to perform a thorough mesh convergence study before the computational analysis.

B. Design of Experiment Table

The design of experiments (DoE) methods are primarily applied using MATLAB R2021a, as reported by previous researchers [11]. The central composite design (CCD) approach is used to create coded variables, which are then used to design the experiment. The coded variables are then decoded to reveal the actual values of the design components [13]. The central composite design (CCD) method was chosen for this study on purpose because of its many benefits, including its speed and efficiency. The implementation of CCD streamlines the research process, resulting in reduced time requirements without compromising the efficacy of experimental design and interpretation [14].

The CCD values were generated in MATLAB R2021a and are shown in Fig. 2. The Coded Variables Matrix (-1, 0, and 1) displays the parameters' minimum, mean, and maximum values, respectively. Every row of the matrix is a unique combination of parameter values to be tested. This structured approach highlights MATLAB's generation of the coded values. Using CCD, this study adopts a well-organized yet effective method for examining the seven key front-end parameters. Maintaining balance between accuracy and feasibility, the analysis delves deeply into the parameters while conserving practicality.

```

Command Window
>> dcc = ccdesign (7, 'type', 'faced')

dcc =

    -1    -1    -1    -1    -1    -1    1
    -1    -1    -1    -1    -1    1    -1
    -1    -1    -1    -1    1    -1    -1
    -1    -1    -1    -1    1    1    1
    -1    -1    -1    1    -1    1    1
    -1    -1    -1    1    1    -1    1
    -1    -1    -1    1    1    1    -1
    -1    -1    1    -1    -1    -1    -1
    -1    -1    1    -1    -1    1    1
    -1    -1    1    -1    1    1    1
    -1    -1    1    -1    1    -1    -1
    -1    -1    1    1    -1    1    -1
    -1    -1    1    1    -1    -1    1
    -1    -1    1    1    1    -1    -1
    
```

Fig. 2. CCD value generated from MATLAB R2021a.

More precisely, in the table provided in Table II, the term x₁ represents the length of the windshield for a sedan car. The lower bound for x₁ is 29 mm, the middle value is 34.5 mm, and the upper bound is 40mm. The coded values enable to represent and analyses the range of the parameter, allowing for convenient interpretation and comparison within the experimental context [11].

Table II. Uncoded parameter analysis: minimum, median, and maximum values.

Parameter	Minimum (-1)	Median (0)	Maximum (1)
x ₁ - WSα (Deg)	29	34.5	40
x ₂ - BL	10	30	50
x ₃ - BCH	435	475.5	516
x ₄ - HLE	50	100	150
x ₅ - HL	635	917.5	1200
x ₆ - Hα (Deg)	11	14.5	18
x ₇ - HEH	565	702	839

C. Computer Aided Design (CAD) Model

The previous researchers generated 79 models and redesigned them in CATIA V5R21 [11]. The CATIA V5R21 models were then exported to .stp file format for ANSYS 2024 R1 analysis. This standardized approach allows design and analysis to be coupled as closely as possible while maintaining their functional grouping.

The profile modelling procedure is simple and repeatable, making it very suitable for creating large numbers of models. It is important that the design of the vehicle in the program is equivalent to a dimension of a sedan car to minimize the errors in drag coefficient calculations. Every single value for the drag coefficient is carefully investigated to find the best design, subject to proper aerodynamic efficiency accomplished for the sedan [15]. This painstaking process boosts cars performance and reliability, making them smoother and more functional on the road.

D. Simulation Set Up

The sedan vehicle model was designed using CATIA V5R21 and thereafter imported into ANSYS 2024 R1 for conducting simulations. ANSYS is then discretizing or creating a mesh around the vehicle model that resembles the flow domain. It represents the volume of air around the vehicle for the simulation. While performing the simulation, it maintains a high level of the physical simulation of the fluid domain, which in turn aids in the aerodynamic assessment of the vehicle application [16].

A fluid volume or enclosure is created to imitate the wind around the vehicle. The enclosure, serving as the airspace, is configured to the conventional dimensions of three car lengths in each dimension: in front of the car, above the car, and beside the automobile, with each side measuring 12,600 mm (equivalent to 3 car lengths). Furthermore, 12,600 mm of clearance is kept between the back of the vehicle and the enclosure's end [17].

Details View	
Details of Enclosure1	
Enclosure	Enclosure1
Shape	Box
Number of Planes	0
Cushion	Non-Uniform
<input type="checkbox"/> FD1, Cushion +X value (>0)	12600 mm
<input type="checkbox"/> FD2, Cushion +Y value (>0)	12600 mm
<input type="checkbox"/> FD3, Cushion +Z value (>0)	12600 mm
<input type="checkbox"/> FD4, Cushion -X value (>0)	12600 mm
<input type="checkbox"/> FD5, Cushion -Y value (>0)	12600 mm
<input type="checkbox"/> FD6, Cushion -Z value (>0)	100 mm
Target Bodies	All Bodies

Fig. 3. Enclosure setup value.

The fluid enclosure dimensional setup is shown in Fig. 3, outlining the proportions and layout of the enclosure.

Once the enclosure has been defined, the next step is to create a mesh. In this process, the fluid domain and vehicle model are divided into small pieces. The accuracy of the simulation directly depends on the quality of the mesh, which ensures the resolution of the flow interactions with higher accuracy. A smoothing routine then refined the mesh structure,

realigning element form for heightened accuracy. Further, local intensification in resolution around the sedan augmented fidelity when assessing aerodynamic traits. The complex mesh was used in the computer simulation to accurately represent the vehicle's lift and drag forces, which let changes to the design be tested to see which ones would improve performance while the vehicle was moving.

E. Mesh Convergence

Mesh convergence analysis is an important step in validating the simulation results of this investigation. It requires the examination of various mesh resolutions so that the results, such as the drag coefficient (Cd), become independent of further refinement. This is a trade-off between accuracy and cost in computation time.

Initially, the element size was defaulted to 2 m for the simulation, then it was divided by two on each successive iteration (1 m, 0.5 m, and more) and the simulation was performed to compare the drag coefficient results for each resolution. Through this comparison, we can identify the mesh that produces accurate results, thereby avoiding the need to compute excess mesh cost. This guarantees that the aerodynamic simulations produce consistent and stubborn values independent of the mesh refinement.

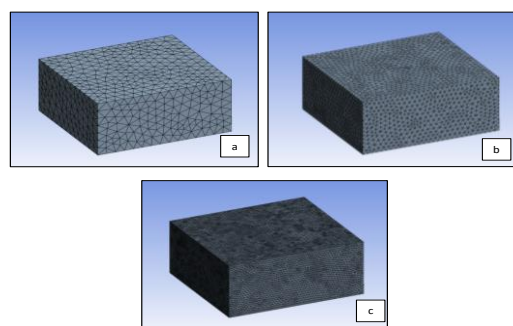


Fig. 4. (a) 2 m element size, (b) 1 m element size, (c) 0.5 m element size.

This analysis employs a variety of mesh resolutions as shown in Fig. 4.

- Figure 4(a) shows the mesh with the largest element size (2 meters), which represents a coarse resolution.
- Figure 4(b) represents the 1-meter mesh, provides a greater resolution than the first.
- Figure 4(c) depicts the finest mesh resolution of 0.5 meters, more detailed airflow interactions around the vehicle to be captured.

This visual comparison highlights how increasing mesh density enhances the detail of the simulation, crucial for accurately evaluating aerodynamic performance. By methodically analysing the impact of these varying mesh resolutions on the drag force coefficient, the study confirms that the selected mesh resolution promotes both computational efficiency and scientific integrity.

III. RESULTS AND DISCUSSION

The dataset employed in this work is derived from a previous study [11, 12] targeting the seven critical parameters highlighted in the Materials and Methods section. To study exclusively the effect of frontal styling on drag, the rear end of the vehicle specifications was kept constant. This indicates that the results of the investigation are attributable to changes in the front-end geometry only. Figure 5 illustrates the diversity of designs chosen that emphasize unique frontal features.

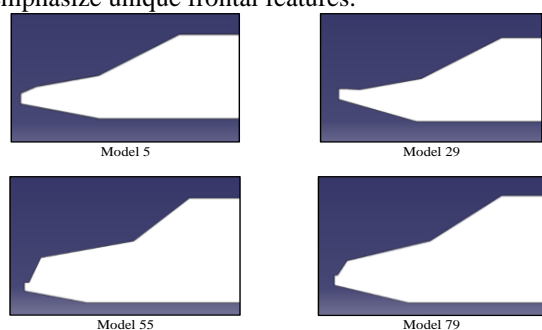


Fig. 5. Selected frontal models.

Table III displays the main dimensional characteristics of four selected car front-end models created with the CATIA program. These models are 5, 29, 55, and 79, showing a variety of frontal profiles intended for analysis of their effects on aerodynamic performance.

Table III. Dimensional specifications of selected vehicle Front-End Models.

Model	x1	x2	x3	x4	x5	x6	x7
5	29	10	435	150	635	11	565
29	29	50	516	150	635	11	565
55	40	50	435	150	1200	11	839
79	34.5	30	475.5	100	917.5	14.5	702

This model is essential for understanding how changes in design relate to aerodynamic performance. This analysis accurately shows the effects of each individual element while keeping the computations simple by only looking at a representative range of designs. The figures highlight unique frontal profiles, underscoring the diversity of the data set and ensuring that the results are representative of a range of designs.

A. Comparison of Mesh Convergence Between Full and Half Models

Table IV. Mesh convergence of Model 5 for full model and half model.

Model	Model 5											
	50 km/h				80 km/h				108 km/h			
	Half Model		Full Model		Half Model		Full Model		Half Model		Full Model	
	Cd	Time										
Default element size (2m)	0.22193 (87 iterations)	54 s	0.24035 (128 iterations)	24 s	0.22124 (88 iterations)	18 s	0.23989 (125 iterations)	18 s	0.22078 (88 iterations)	31 s	0.23967 (125 iterations)	29 s
Default element size (1m)	0.32502 (126 iterations)	42 s	0.28121 (139 iterations)	55 s	0.32849 (136 iterations)	28 s	0.27253 (135 iterations)	36 s	0.33664 (144 iterations)	28 s	0.26947 (136 iterations)	56 s
Default element size (0.5m)	0.28818 (60 iterations)	390 s	0.20588 (76 iterations)	449 s	0.28986 (59 iterations)	373 s	0.20536 (77 iterations)	335 s	0.28751 (59 iterations)	627 s	0.20499 (78 iterations)	393 s

The drag coefficient values were derived through simulations, allowing for a thorough comparison between the full and half models. The comparison, as delineated in the Table III, was carried out at different velocities: The speed of 50 km/h is a critical safety measure for pedestrians. The speed of 80 km/h is regularly encountered on roads. The speed of 108 km/h is typically noticed on highways and represents higher velocities. The comparison of drag coefficient values between the two model types at these specific speeds offers useful insights into the aerodynamic efficiency of the vehicles under varying operational circumstances. In this study, a homogenous mesh was selected instead of an adaptive mesh with the interest of maintaining numerical consistency. An adaptive mesh may improve computational efficiency with refinements in regions of high gradient but may cause additional complexities in refinement. With the use of uniform mesh, a better control over element quality is achieved and solver stability is maintained.

Figure 6 shows the geometric distinctions between the full and half models, with the first one representing the complete vehicle and the second one concentrating just on its front end. Table IV allows the study of Model 5 to show important developments in aerodynamic accuracy and computational efficiency.

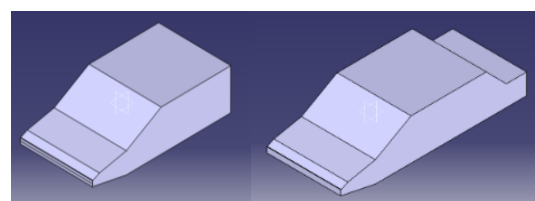


Fig. 6. Model 5 for half model and full model.

Ideally, the drag coefficient (C_d) would be lower when using the full model instead of the partial one. Nevertheless, this tendency is unstable for a 2m element size over all speeds (50 km/h, 80 km/h, and 108 km/h), either because of coarse mesh resolution, solver convergence problems, or numerical instability. While preserving adequate calculation time (449s vs. 390s), the full model achieves a notably lower C_d (0.20588 at 50 km/h) at a finer 0.5 m element size than the half model (0.28818). Despite a marginal improvement in runtime, the half model's greater C_d indicates diminished accuracy.

Table VI. Mesh convergence of Model 29 for full model and half model.

Model	Model 29											
	50 km/h				80 km/h				108 km/h			
	Half Model		Full Model		Half Model		Full Model		Half Model		Full Model	
	Cd	Time										
Default element size (2m)	0.52822 (138 iterations)	17 s	0.24098 (146 iterations)	25 s	0.53064 (150 iterations)	36 s	0.24167 (148 iterations)	35 s	0.53432 (137 iterations)	11 s	0.23784 (147 iterations)	17 s
Default element size (1m)	0.35298 (84 iterations)	52 s	0.26480 (94 iterations)	89 s	0.35332 (86 iterations)	73 s	0.25899 (96 iterations)	76 s	0.35294 (88 iterations)	71 s	0.25210 (98 iterations)	71 s
Default element size (0.5m)	0.31102 (63 iterations)	450 s	0.21458 (63 iterations)	481 s	0.31165 (64 iterations)	654 s	0.21612 (65 iterations)	440 s	0.31222 (63 iterations)	845 s	0.21638 (64 iterations)	373 s

Computational time does not follow the expected trend, where decreasing element size should decrease Cd, lower iterations, and increase time. At a 2 m element size, Table IV shows that the lower iteration counts still take longer to compute, possibly due to the not considering the turbulence of the model.

Table V. Mesh Density Comparison for Model 5.

Element size	Model 5			
	Half Model		Full Model	
	Nodes	Elements	Nodes	Elements
2 m	2034	9589	2133	10032
1 m	10379	52386	11031	55974
0.5 m	50415	263194	50988	265981

Table V shows that reducing the mesh from 2 m to 0.5 m greatly increases the number of nodes and elements for both models; with the full model always having somewhat higher values because of its broader computational domain. Although it increases computing cost, this increase enhances accuracy and supports the whole dependability of the model for exact aerodynamic simulations.

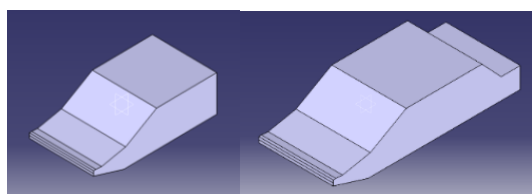


Fig. 7. Model 29 for half model and full model.

Emphasizing their different simulated configurations, Fig. 7 shows the geometric variations between the full and half models of Model 29. Table VI shows the drag coefficient (Cd) and computing time analyses across several speeds; usually,

decreasing the element size increases computation time. However, in particular at a 0.5 m element size, the full model shows more stability and consistency.

Although the half model has the same element size, it generates a higher Cd of 0.31165 and requires 654 seconds, taking far more time and producing less accurate results than the complete model obtains at 80 km/h in 440 seconds. This runs counter to the expected trend, probably resulting from solver inefficiencies or numerical instability that the half model should estimate faster. The whole model's constantly reduced Cd values at various speeds highlight even more its aerodynamic accuracy's excellence.

Table VII. Mesh density comparison for Model 29.

Element size	Model 29			
	Half Model		Full Model	
	Nodes	Elements	Nodes	Elements
2 m	2074	9803	2161	10164
1 m	10396	52508	11072	56196
0.5 m	50468	263560	50963	265797

Refining the mesh from 2 m to 0.5 m greatly increases the number of nodes and elements for both models based on Table VII, Mesh Density Comparison for Model 29 with the full model constantly having somewhat higher values due of its broader computational domain. The enhanced simulation precision and increased computing cost are evidence of the entire model's dependability in producing stable and accurate aerodynamic results.

Table VIII. Mesh convergence of Model 55 for full model and half model.

Model	Model 55											
	50 km/h				80 km/h				108 km/h			
	Half Model		Full Model		Half Model		Full Model		Half Model		Full Model	
	Cd	Time										
Default element size (2m)	0.52298 (125 iterations)	7 s	0.33859 (176 iterations)	10 s	0.52305 (135 iterations)	13 s	0.33877 (169 iterations)	11 s	0.52306 (139 iterations)	36 s	0.33888 (171 iterations)	13 s
Default element size (1m)	0.63805 (88 iterations)	112 s	0.32783 (99 iterations)	79 s	0.63993 (93 iterations)	198 s	0.32831 (112 iterations)	77 s	0.61300 (113 iterations)	63 s	0.32834 (113 iterations)	74 s
Default element size (0.5m)	0.38896 (72 iterations)	570 s	0.24527 (77 iterations)	386 s	0.38819 (72 iterations)	555 s	0.24707 (77 iterations)	376 s	0.38978 (72 iterations)	457 s	0.24634 (80 iterations)	606 s

Table X. Mesh convergence of Model 79 for full model and half model.

Model	Model 79											
	50 km/h				80 km/h				108 km/h			
	Half Model		Full Model		Half Model		Full Model		Half Model		Full Model	
	Cd	Time										
Default element size (2m)	0.26353 (61 iterations)	60 s	0.29832 (165 iterations)	47 s	0.26174 (61 iterations)	55 s	0.29884 (166 iterations)	14 s	0.25998 (60 iterations)	43 s	0.28946 (169 iterations)	14 s
Default element size (1m)	0.40730 (131 iterations)	50 s	0.28184 (131 iterations)	63 s	0.41571 (128 iterations)	38 s	0.28102 (134 iterations)	49 s	0.41079 (170 iterations)	22 s	0.28115 (139 iterations)	44 s
Default element size (0.5m)	0.30966 (68 iterations)	508 s	0.23593 (81 iterations)	415 s	0.30975 (66 iterations)	374 s	0.24213 (83 iterations)	348 s	0.30900 (65 iterations)	557 s	0.23717 (83 iterations)	413 s

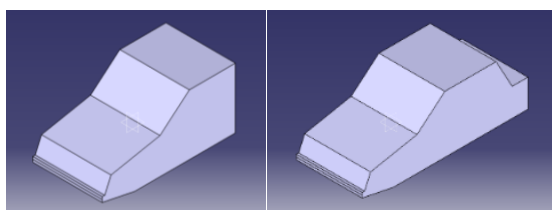


Fig. 8. Model 55 for half model and full model.

Table VIII displays the Model 55's aerodynamic performance at various speeds, which supports the idea that a smaller element size always leads to a lower drag coefficient (Cd). Emphasizing their structural and aerodynamic interactions, Fig. 8 graphically contrasts both the full and half models.

According to the data, the full model with a 0.5 m element size computes a Cd of 0.24707 in 376 seconds at 80 km/h; the half model produces a far higher Cd of 0.38819 in 555 seconds. Likewise, the half model generates 0.38978 in 457 seconds, whereas the full model records a Cd of 0.24634 in 606 seconds at 108 km/h. The entire model's higher accuracy and consistency define it as the more dependable choice for aerodynamic simulations despite little changes in processing time.

Table IX. Mesh density comparison for Model 55.

Element size	Model 55			
	Half Model		Full Model	
	Nodes	Elements	Nodes	Elements
2 m	2108	10010	2207	10472
1 m	10485	52906	11133	56381
0.5 m	54193	284776	53633	280772

Table IX shows the difference in increasing the number of nodes and elements in both the half and full models by lowering the element size from 2 m to 0.5 m. Due to its broader computational domain, which helps to increase simulation accuracy, the complete model always consists of more nodes and elements than the half model. A denser mesh is necessary for more accurate drag coefficient (Cd) calculations, as it reveals the flow characteristics of aerodynamics in greater depth.

A finer mesh raises computational cost even while improving accuracy. Greater memory use and longer processing times follow from the rise in node and element count. Still, the complete model is the recommended alternative since it can produce lower and more consistent Cd values while preserving stability over several speeds. This harmony between

aerodynamic precision and computational cost emphasizes the need for mesh refinement in obtaining consistent simulation results.

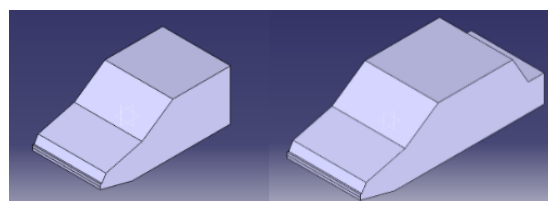


Fig. 9. Model 79 for half model and full model.

Table X briefly shows the drag coefficients (Cd) and computation times for Model 79 at different speeds, which helps us understand the trade-offs between how fast the computations are and how well they match the aerodynamics. Figure 9 graphically shows the entire and half models, thereby accentuating their structural variations. With much reduced Cd values, the research indicates that the whole model routinely beats the half model in terms of accuracy at finer mesh resolutions (0.5 m element size). For example, the half model computes a far higher Cd of 0.30966 in 508 seconds, while the full model obtains a Cd of 0.23593 in 415 seconds at 50 km/h. At 108 km/h, a similar pattern is seen whereby the complete model computes a Cd of 0.23717 in 413 seconds, compared to the Cd of 0.30900 in 557 seconds by the half model.

Nevertheless, anomalies occur at a 2 m element size when the whole model generates a greater Cd than the half model, most likely because of coarse meshing and solver convergence problems. Furthermore, there is no guarantee that a finer mesh will improve computing time; this is especially true in the half model. Solver inefficiency, sensitivity to the turbulence of the model, or numerical instability could all be causes of this inconsistency. Notwithstanding these differences, the complete model is still the recommended alternative for aerodynamic simulations since it guarantees more exact results and preserves computational economy.

Table XI. Mesh density comparison for Model 79.

Element size	Model 79			
	Half Model		Full Model	
	Nodes	Elements	Nodes	Elements
2 m	2028	9539	2177	10279
1 m	10414	52642	11131	56499
0.5 m	51541	268685	53280	279546

Table XI shows Model 79's decreasing element size results in a rise in nodes and elements. Although it increases computational time, the complete model routinely includes more nodes and elements than the half model, therefore boosting accuracy. Lower mesh density at a 2 m element size could result in errors that would raise Cd values in the full model. The 0.5 m mesh makes the models more accurate, but it hurts the solver's performance, especially in the half model where the trends in computational time become less stable.

It is worth noting, however, that reducing the element size from 2 m to 0.5 m results in longer

computation times and an increased accuracy for both models.

Table XII is the display of the percentage difference in Cd for the 1 m and 0.5 m element sizes at a speed of 50 km/h for all four full models analysed:

Table XII. Percentage difference in Cd for the 1 m and 0.5 m element sizes.

Model 5	Model 29	Model 55	Model 79
26.80%	18.97%	25.18%	16.29%

Although the Cd value appears to converge as the element size is reduced, the percentage difference between the 1 m and 0.5 m element sizes remains high.

Table XIII. Mesh convergence of all full models with element sizes 0.3 m and 0.5 m for 50 km/h.

Model	5		29		55		79	
Elements Size (m)	0.3	0.5	0.3	0.5	0.3	0.5	0.3	0.5
Nodes	181407	50988	181469	50963	193391	53633	188615	51541
Elements	975493	265981	975855	265797	1043753	280772	1016752	268685
Time	0:23:34	0:07:23	0:11:57	0:08:22	25:41:00	0:14:25	0:48:07	0:08:50
Iterations	118	76	210	63	104	77	92	81
Drag Coefficient	0.20132	0.20588	0.20685	0.21458	0.24475	0.24527	0.20905	0.23593
Percentage difference in Cd for the 0.5 m and 0.3 m element sizes	2.21%		3.60%		0.21%		11.39%	

To minimize this difference, a smaller element size of 0.3 m is used to analyse all four models at a speed of 50 km/h in the full model design.

B. Further Mesh Refinement: 0.5 m to 0.3 m Element Size

The Table XIII presents data for the full model at a velocity of 50 km/h, comparing the performance of two element sizes, 0.3 m and 0.5 m, across models 5, 29, 55, and 79. Key factors such as nodes, elements, computation time, iterations, and drag coefficient (Cd) and percentage difference in Cd for 0.5 m and 0.3 m element size are analysed, showing how the different element sizes affect the simulation's performance.

Figure 10 compares the drag coefficients (Cd) of Models 5, 29, 55, and 79 at various element sizes (0.3 m, 0.5 m, 1 m, and 2 m). Across all models, smaller element sizes, like 0.3 m and 0.5 m, consistently yield lower drag coefficients, indicating better accuracy in capturing aerodynamic details. As the element size increases, the Cd rises, showing reduced precision with coarser meshes.

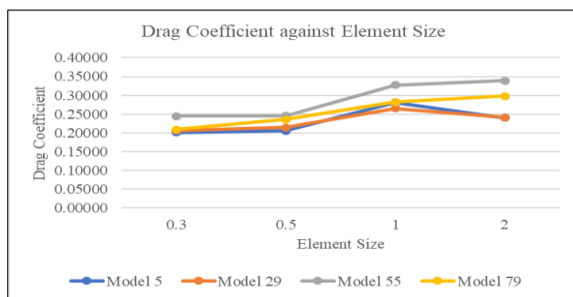


Fig. 10. Graph of Drag Coefficient against element size.

In terms of computational time, the 0.5 m element size is always much better than the 0.3 m element size.

In this case, Model 79, the simulation with the 0.5 m element size, completed in 0:08:50, and the same model with a 0.3 m element size took substantially longer, 0:48:07. It is thus much more efficient with respect to time when using the 0.5 m element size for the aerodynamics simulations, which holds for all models.

The number of iterations needed indicates how effective the 0.5 m element size is. As an example, Model 29 took 63 iterations to finish the simulation with the 0.5 m element size, while it needed 210 iterations with the 0.3 m element size. Less the number of iterations results in less the overall computational cost associated with it, and it thus facilitates a great trade-off, which is in the case of balancing computational resources with simulation needed in the favour of 0.5 m element size elements.

Although the drag coefficient values associated with the 0.3 m element size are slightly more accurate, the difference is minor. For example, Model 5 Cd is 0.20132 for the 0.3 m element size and 0.20588 for the 0.5m element size. For the 0.3 m element size, the increase in accuracy does not outweigh the increase in processing time and resources required. The Table IX also provides important insights into the number of nodes and elements, which are key indicators of mesh resolution. As expected, the 0.3 m element size produces significantly more nodes and elements than the 0.5 m size across all full models, which directly impacts computational requirements.

For instance, in Model 5, the 0.3 m element size generates 181,407 nodes and 975,493 elements, whereas the 0.5 m size produces only 50,988 nodes and 265,981 elements. This reduction in nodes and elements with the 0.5 m element size is consistent across all models. In Model 79, for example, the 0.3 m size yields 188,615 nodes and 1,016,752 elements,

compared to 51,541 nodes and 268,685 elements for the 0.5 m size.

This significant difference in mesh density explains the longer computation times associated with the 0.3 m element size. A finer mesh (more nodes and elements) increases simulation accuracy but at the cost of dramatically higher computational load. Conversely, the 0.5 m element size offers a coarser mesh, which reduces the computational burden while still delivering reliable results.

Although the 0.3 m element size provides a higher level of detail in the mesh, the trade-off is a substantial increase in the number of nodes and elements, leading to longer processing times. The 0.5 m element size, while coarser, strikes a more efficient balance between mesh resolution and computation time. Therefore, the 0.5 m element size is often preferred in simulations, as it provides enough accuracy without the excessive computational overhead associated with finer meshes [17].

In terms of accuracy, while the 0.3 m element size produces slightly lower Cd values (which suggests higher accuracy), the percentage difference between the two sizes is relatively small for most models. For Model 5, the percentage difference in Cd is 2.21%, while in Model 29 it is 3.60%. While Model 55 showed minimal variation with only a 0.21% difference between element sizes, Model 79 demonstrated notable divergence with a hefty 11.39% gap. Even though there was a bigger difference in percentages in Model 79, using the 0.5 m element size continued to save time and require fewer iterations, making it the clear choice. Moreover, the general precision remained within tolerable limits of error typically between 5-10% for most models. Model 79 has only a slightly higher error than 10% indication a possible local deviation attributed to possible factor like turbulence model limitations or inadequate mesh resolution.

Overall, the full model using 0.5 m elements at 50 km/h strikes the best compromise between accuracy and speed. Although the Cd values are much lower for the 0.3 m size, the 0.5 m element size has been selected for the aerodynamic simulation due to its significantly lower computational time, fewer iterations, and overall efficient calculations.

C. Convergence Analysis of ANSYS Simulation: Residual Behaviour and Iteration Performance

The residual convergence plots for Models 5, 29, 55, and 79 show how well each configuration works in the same conditions: a full model prototype moving at 50 km/h with an element size of 0.5 meters. Key flow variables, such as continuity, velocity vectors, and turbulence properties, coming together shows how steady and accurate the re-enactment is. Each model's air resistance coefficient varies, demonstrating the impact of front-end style on aerodynamic functionality. The examination starts with the streamlined Model 5 and continues through the more complex Models 29, 55, and 79, exploring how each form influences convergence behaviour and the general simulation proficiency.

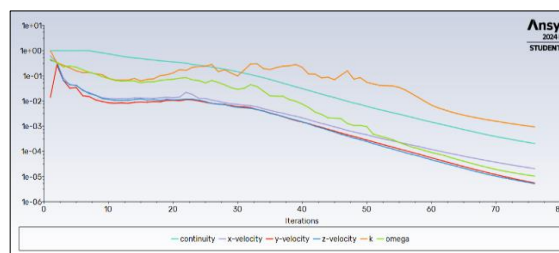


Fig. 11. Residual convergence plot of Model 5.

Residual convergence behaviour of Model 5 at 50 km/h at 0.5 m element size is shown in Fig. 11. Residuals of important variables in terms of continuity, velocity components in the x, y, and z directions, and turbulence, k, and omega are shown over 80 iterations in the graph. The continuity residual (shown in a light blue line) starts high but continues dropping steadily, nearing $1e^{-4}$ by the end of the iterations, which is a sign that the flow field has mostly converged. The residuals in the x-velocity (purple line), y-velocity (red line), and z-velocity (blue line) also collapse nicely, dropping to values close to $1e^{-5}$, signalling that the velocity fields are resolving accurately.

The turbulence parameters k (the orange line) and omega (the green line) show different convergence behaviours. The omega residual decreases smoothly, reaching $1e^{-5}$, while k takes longer to converge, with residuals around $1e^{-2}$ by iteration 80. This indicates that while the velocity fields and continuity are well-converged, the turbulence energy dissipation (k) is slower to reach convergence. In general, the graph indicates that the simulation under Model 5 is converging reasonably well, with some potential for further k parameter improvements. An increase in the number of iterations might be beneficial to reach more stable values of turbulence parameters and consistency of the simulation [18].

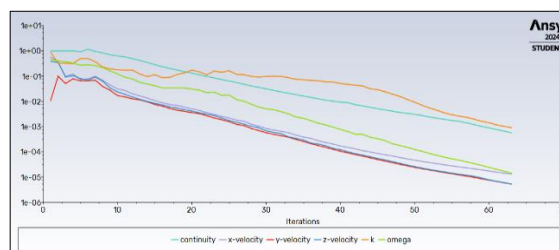


Fig. 12. Residual convergence plot of Model 29.

Figure 12 shows the convergence trends for Model 29, which was simulated in the same conditions as Model 5 at a speed of 50 km/h and a component size of 0.5 meters. The graph demonstrates the residuals for crucial factors, like continuity, velocity elements (x, y, and z directions), and turbulence parameters (k and omega), over 70 iterations. At first, the continuity residual (light blue line) is elevated, but it progressively shrinks, approaching $1e^{-3}$ by the end of the iterations. This development indicates the significant stabilization of the current field. The residuals for x-speed (in purple), y-speed (in red), and z-speed (in blue) also exhibit commendable

convergence, eventually settling near $1e^{-5}$, which suggests a precise resolution of the velocity fields.

However, the turbulence parameters k (orange line) and ω (green line) show completely different convergence behaviour. While the ω residual steadily declines, reaching $1e^{-5}$, the k parameter lags and maintains residuals around $1e^{-3}$ by the final iteration. This observation signifies that, although the velocity fields and continuity are effectively converged, the turbulence energy dissipation parameter (k) needs further iterations to stabilize. Overall, it can be seen from the graph that the simulation for Model 29 is going to converge.

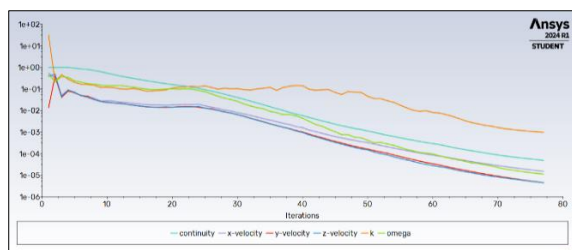


Fig. 13. Residual convergence plot of Model 55.

In the ANSYS simulation of Model 55 (full model) at 50 km/h and 0.5 m element size, Fig. 13 shows how the different flow variables (continuity, x-velocity, y-velocity, z-velocity, k , and ω) slowly came together. The graph illustrates the residuals over 80 iterations, providing insights into the simulation's convergence toward a stable solution.

All the residuals show a general reducing trend, which is an indication of positive convergence. The continuity residual (light blue line) began with relatively high values and gradually decreased throughout, reaching a value of $1e^{-4}$ by iteration 70. This suggests that the continuity equation solution is approaching stability, even though it remains higher than other factors.

The velocity parts—x-velocity (purple line), y-velocity (red line), and z-velocity (blue line)—demonstrated a smoother decline, with residuals steadily falling. By iteration 80, these values approached $1e^{-5}$ to $1e^{-6}$, signifying that the velocity fields were well-converged and highly precise. These fluid patterns are key to capturing flow dynamics accurately.

The turbulence parameters k (orange line) and ω (green line) represent energy dissipation and turbulence behaviour, respectively, using the k - ω turbulence model. While ω demonstrated excellent convergence with residuals decreasing to around $1e^{-5}$, k maintained higher residuals throughout the iterations. By iteration 70, k remains at $1e^{-2}$, suggesting that the turbulence dissipation rate converges at a slower pace. This progression is commonly seen in k - ω modelled simulations, as turbulence properties frequently necessitate additional iterations to stabilize.

The overall convergence of the simulation is promising. While the results show a reduction in residuals over most variables and therefore a stabilisation of the solution, continuity and k residuals

are still relatively high compared to the values of velocity and ω . This implies that additional accuracy iterations could specifically benefit these parameters. The smoothness of the graph also indicates numerical stability, suggesting that the mesh, boundary conditions, and solver settings have been optimally defined for this simulation [19, 20].

This history of iterations shows that the ANSYS simulation of Model 55 is on the right track to resolution, with the turbulent kinetic energy and velocity elements coming together correctly. While the residuals for continuity and k remain higher than preferred, the calculation appears stable and dependable. Increasing the iteration count beyond 80 may help achieve better results, especially in the case of more realistic turbulent flow models, and it would result in more accurate aerodynamic predictions.

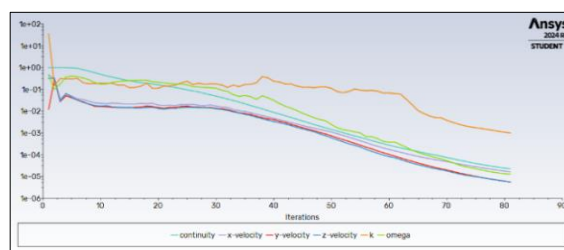


Fig. 14. Residual convergence plot of Model 79.

Figure 14 depicts the residuals for Model 79, tested at 50 km/h with an element size of 0.5 meters. The chart illustrates the behavioural patterns of key flow factors, including continuity, velocity aspects (x, y, and z), and turbulence principles (k and ω) across 90 cycles, providing insights into the simulation's progression toward a stable resolution.

A steady descending tendency in residuals signifies compelling convergence. The continuity residual (light blue line) is heightened but reliably declines, nearing $1e^{-4}$ by iteration 80, indicating a propensity toward stability, though it remains somewhat elevated compared to other variables. The residuals for the speed aspects, which are x-speed (purple line), y-speed (red line), and z-speed (blue line), show a smoother decrease that converges to around $1e^{-5}$ by iteration 80, which means that the velocity fields are very accurate.

The turbulence benchmarks k (the orange line) and ω (the green line) epitomize energy dissipation and turbulence qualities, respectively, as modelled by the k - ω approach. The ω residual demonstrates good convergence, reaching around $1e^{-5}$, whereas k remains higher at about 0.1 by iteration 80, suggesting slower stabilization, which is typical for k - ω simulations.

While most residuals pointed to stabilization overall, the higher values for continuity and K implied room for refinement through extra cycles. The plot's fluidity signalled numerical stability, suggesting the mesh, boundary conditions, and problem solver conditions were appropriately tuned. So, the ANSYS modelling of Design 79 seemed to be making good progress towards convergence. Further iterations could lead to better representations of turbulence,

which would improve the accuracy of the aerodynamic predictions.

When carrying out an analysis using ANSYS, the time demanded to agree on a solution is directly proportional to the number of iterations that are performed. Generally, a greater number of iterations will lengthen processing durations, particularly for simulations that are more intricate. Nonetheless, augmenting the quantity of iterations can enhance the precision by enabling the solver to progressively enhance the solution until it reaches a stable outcome [21].

The above findings exhibit marked differences in the iteration count across diverse element sizes and designs. For example, when compared to the full model or models with larger element sizes, the half model with a smaller element size typically requires a higher number of iterations to reach convergence. The basis behind this is that when element sizes are reduced, the mesh becomes more intricate, which in turn compels the solver to perform more calculations to accurately capture the stream's behaviour [22].

Varying the number of iterations can improve correctness, but it also brings about extended processing time. Hence, there is often a compromise between precision and computational potency [23]. Striking a balance between minimizing processing assets and attaining appropriate accuracy is pivotal in practical simulations.

IV. CONCLUSION

The present study sought to find the ideal mesh size for computational simulations involving numerous sedan automobile types while assessing front-end effects on aerodynamic efficiency. The main goal of the study was to find the most effective mesh arrangement balancing computing time and accuracy in drag coefficient (Cd) observations. The results showed that the ideal trade-off between accuracy and computational economy is provided by a 0.5 m element size.

A secondary aim was to conduct a comparison of full and half models. The results show that although the half model usually uses fewer computing resources, the full model consistently and accurately yields Cd values. So, for future computational fluid dynamics (CFD) studies, a full model would be better because it keeps the back-end structure the same, which makes the aerodynamic assessment more accurate.

However, a limitation of this study is that it only accounts for changes at the front end while maintaining the rear of the car unchanged. Future studies should look into how different rear-end shapes affect aerodynamic performance. Additional research into the refinement of mesh-refining procedures could also be performed to provide more precision in simulation while not providing an extreme burden on computing. In addition, it is also recommended that wind tunnel tests be carried out as part of the experimental validation of CFD results to strengthen the reliability of numerical findings.

ACKNOWLEDGEMENT

This research is not funded.

REFERENCES

- [1] M. G. Connolly, A. Ivankovic and M. J. O'Rourke, "Drag Reduction Technology and Devices for Road Vehicles - A Comprehensive Review," *Heliyon*, vol. 10, no. 13, pp. e33757, 2024.
- [2] B. C. Ismail and U. Ghia, "Procedure for Estimation and Reporting of Uncertainty Due to Discretization in CFD Applications," *J Fluids Eng.*, vol. 130, no. 7, pp. 078001, 2008.
- [3] M. Schlipf, A. Tismer and S. Riedelbauch, "On the Application of Hybrid Meshes in Hydraulic Machinery CFD Simulations," in *IOP Conf. Series: Earth and Environ. Sci.*, vol. 49, pp. 062013, 2016.
- [4] M. L. Mohamad, M. T. A. Rahman, S. F. Khan, M. H. Basha, A. H. Adom and M. S. M. Hashim, "Design and Static Structural Analysis of A Race Car Chassis for Formula Society of Automotive Engineers (FSAE) Event," *J. Physics: IOP Conf. Series*, vol. 908, pp. 012042, 2017.
- [5] A. R. Prabowo, B. Cao, J. M. Sohn and D. M. Bae, "Crashworthiness Assessment of Thin-Walled Double Bottom Tanker: Influences of Seabed to Structural Damage and Damage-Energy Formulae for Grounding Damage Calculations," *J. Ocean Eng. and Sci.*, vol. 5, no. 4, pp. 387–400, 2020.
- [6] A. Ghavidel, M. Rashki, H. G. Arab and M. A. Moghaddam, "Reliability Mesh Convergence Analysis by Introducing Expanded Control Variates," *Front. Structur. and Civ. Eng.*, vol. 14, no. 4, pp. 1012–1023, 2020.
- [7] C. Shah, "Mesh Discretization Error and Criteria for Accuracy of Finite Element Solutions," *Scribd*, pp. 1-12, 2018.
- [8] A. Bepalov, A. Haberl and D. Praetorius, "Adaptive FEM with Coarse Initial Mesh Guarantees Optimal Convergence Rates for Compactly Perturbed Elliptic Problems," *Comput. Methods Appl. Mech. Eng.*, vol. 317, pp. 318–340, 2017.
- [9] C. Gao, "Effect of Front Windshield Angle on Drag Coefficient of Electric Vehicles," *Theoret. and Nat. Sci.*, vol. 12, no. 1, pp. 101–107, 2023.
- [10] S. Vignesh, V. S. Gangad, V. Jishnu, Maheswarreddy, A. Krishna and Y. S. Mukkamala, "Windscreen Angle and Hood Inclination Optimization for Drag Reduction in Cars," in *Proc. Manufactur.*, pp. 685–692, 2019.
- [11] V. Kausalyah, S. Shasthri, K. A. Abdullah, M. M. Idres, Q. H. Shah and S. V. Wong, "Optimisation of Vehicle Front-End Geometry for Adult and Pediatric Pedestrian Protection," *Int. J. Crashworthiness*, vol. 19, no. 2, pp. 153–160, 2014.
- [12] Y. Mizuno, "Summary of IHRA Pedestrian Safety Working Group Activities (2005) Proposed Test Methods to Evaluate Pedestrian Protection Afforded By Passenger Cars," *Baidu*, 2005.
- [13] S. Bhattacharya, "Central Composite Design for Response Surface Methodology and Its Application in Pharmacy," *Respon. Surf. Methodol. in Eng. Sci.*, pp. 1-19, 2021.
- [14] V. Kausalyah, M. S. Shafiq and S. Shasthri, "Analysis of The Influence of The Rear End Sedan Vehicle Profile on The Aerodynamic Efficiency," *ARPN J. Eng. and Appl. Sci.*, vol. 15, no. 13, pp. 1412-1419, 2020.
- [15] E. Abo-Serie, A. Gaylard and N. E. Ahmad, "Mesh Optimization for Ground Vehicle Aerodynamics," *CFD Lett.*, vol. 2, no. 1, pp. 54-65, 2010.
- [16] J. Broniszewski and J. Piechna, "A Fully Coupled Analysis of Unsteady Aerodynamics Impact on Vehicle Dynamics During Braking," *Eng. Appl. Computat. Fluid Mechan.*, vol. 13, no. 1, pp. 623–641, 2019.
- [17] A. S. Mahdi Al-Obaidi and L. C. Sun, "Calculation and Optimization of The Aerodynamic Drag of An Open-Wheel Race Car," *EURECA*, pp. 29-30, 2013.
- [18] M. K. Thompson and J. M. Thompson, "Meshing," *ANSYS Mechanical APDL for Finite Element Analysis*, pp. 181–199, Elsevier Science, 2017.

- [19] O. Persson, "Mesh Generation for Implicit Geometries," *PhD Thesis*, MIT, 2004.
- [20] O. Ogundairo, "Adaptive Mesh Refinement in Numerical Methods for Fractional Differential Equations," *Scribd*, pp. 1-32.
- [21] G. Zumbusch, "Parallel Multilevel Methods," *Advances in Numerical Mathematics*, Springer, 2003.
- [22] M. Aultman, Z. Wang and L. Duan, "Effect of Time-step Size on Flow Around Generic Car Models," *J. Wind Eng. and Industr. Aerodynam.*, pp. 104764, 2021.
- [23] S. Ereiz, I. Duvnjak and J. F. Jiménez-Alonso, "Review of Finite Element Model Updating Methods for Structural Applications," *Structures*, vol. 41, no. 1, pp. 684-723 2022.